Substitution Behavior and Electronic Modification of Quadruply-Bonded Complexes of Molybdenum and Tungsten

A Senior Honors Thesis

Presented in Partial Fulfillment of the Requirements for Graduation
with Distinction in Chemistry in the Undergraduate Colleges
of The Ohio State University

by

Christopher William James Gribble

Project Adviser: Professor Malcolm H. Chisholm, Department of Chemistry

Table of Contents

ABSTRACT

$W_2(mhp)_4$ was examined as a starting material for the synthesis of the evasive ditungsten tetracarboxylates with the following carboxylic acids: 2-thienylcarboxylic acid, benzoic acid, 9-anthracenylcarboxylic acid (Anth-9-CO_2H), and 2,4,6-triisopropylbenzoic acid (TiPB). It was determined that the reaction of $W_2(mhp)_4$ and Anth-9-CO_2H provides a convenient preparatory method for a $W_2(O_2CR)_4$ complex.

The synthesis of the series, $Mo_2(mhp)_{4-x}(TiPB)_x$ (where x = 1-4), was attempted to illustrate the ability to selectively modify the electronic structure of paddlewheel complexes. The complexes corresponding to x = 0, 1, 2, and 4 have been synthesized and UV-vis results implicate the ability to control electronic features via stepwise mhp-carboxylate ligand substitution.

Dimolybdenum paddlewheel complexes were linked with both 2,5-thienyldicarboxylate and 3,4-thienyldicarboxylate as an attempt to probe the effect that linker geometry has on the electronic properties of the coupled "dimers of dimers". The complexes were characterized via electrochemical methods and UV-vis spectroscopy.

The complex, $[Mo_2(mhp)_2(CH_3CN)_4][BF_4]_2$, has been synthesized and its structure has been determined by single crystal X-ray crystallography. The reaction of this dication with a dicarboxylate salt was determined to yield a mixture of molecular triangles and squares by mass spectrometry.

CHAPTHER 1

INTRODUCTION

1.1 Introductory remarks

The phenomenon of carbon-carbon and carbon-heteroatom multiple bonds is a concept familiar to all of those whom have taken even the most introductory of chemistry courses. The organic chemist has long since exploited the reactivity of these functionalities to enact a wide variety of chemical transformations. That stated, the concept of metal-metal multiple bonds was not recognized until the early 1960's with the quadruple bond being much more elusive, evading the minds of chemists until Cotton's thorough structural characterization of the rhenium chloride anion, $[Re_2Cl_8]^{2-}$. The metal-metal multiple bond is now a common motif in systems with transition metals in low oxidation states supported by stabilizing organic ligands.[1]

While multiple bonds between first row elements are thermodynamically stable, the same is not necessarily true for heavier elements, which is a direct consequence of the size of the element's inner core.[2] The unique stability of multiple bonds between first row elements can be rationalized by considering the size of the small helium inner core. Multiple bonds between transition metal atoms are favored by kinetic factors and often require the use of sterically demanding ligands, which raise the activation barrier to cluster formation.[2] In contrast to the chemistry of the main group elements, (sp block), metal-metal bonding strength increases down a group for the transition elements as a result of the greater radial extension of the 5d>4d>3d orbitals. Thus MM multiply

bonded complexes are more common for the 2nd and 3rd row transition elements. Complexes of this type often adopt a paddlewheel conformation as shown in Figure 1 (see below). A variety of bridging ligands have proven quite useful in this regard with carboxylates being the most commonly employed.

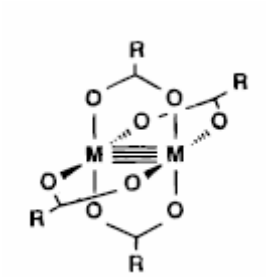

Figure 1.1 Paddlewheel conformation for a generic carboxylate-stabilized quadruply bonded dimetal complex (Extract from Ref. 3).

1.2 Advantages of carboxylates as supporting ligands

The widespread use of carboxylate anions as bridging ligands in paddlewheel complexes can be attributed to several factors including kinetic lability and solubility. Dimetal tetracarboxylates are excellent starting materials for the synthesis of mixed-ligand species and higher order assemblies because of the ease in which the carboxylates can be substituted. Furthermore, the relative solubility of the dimetal tetracarboxylates can be systematically varied as a function of the R group on the carboxylate backbone (See Figure 1 above), with long aliphatic substituents increasing solubility in hydrocarbon solutions.

1.3 Disadvantages of carboxyates as supporting ligands

While the use of bridging carboxylate anions in paddlewheel complexes is advantageous in some respects, their use is also accompanied by some inherent disadvantages. This is particularly true with respect to geometry preservation whereby the lability of the carboxylate anions encourages ligand scrambling.[4,5] Thus, dimetal systems supported by carboxylate ligands are often dynamic in solution. While this is not a problem in homoleptic systems, it can be a limiting factor in mixed-ligand systems and higher order assemblies. Geometry fixation in mixed-ligand paddlewheel complexes is often only obtainable in the limit that the desired species serves as a thermodynamic sink or in processes where the kinetic barrier leading to desired species is significantly lower than that for the other isomers. This is usually the case for bis-bis dimetal complexes with two very sterically demanding ligands and two much smaller ligands.

Furthermore, the ability to rigorously control geometric parameters becomes increasingly important in the synthesis of higher order assemblies incorporating dimetal cores, especially with respect cyclic oligomers, i.e. molecular triangles and squares. A common strategy in this regard includes the design of stereochemically rigid, reactive templates for the use in directed self-assemblies. The directed synthesis of cyclic oligomers requires the use of cis-directing templates. The design of rigorously cis-directing units is accomplished by the use of ligands bolstering a strong trans influence. Carboxylates are weakly trans influencing ligands, and hence, are poor candidates for the synthesis of cyclic oligomers. On the other hand, most ligands bearing nitrogen donors provide a significant trans influence, i.e. formamidinates and amidinates, thus allowing the design of cis- directing units.

1.4 Bonding analysis of group 6 dimetal paddlewheel complexes

Perhaps, the most well understood quadruply bonded paddlewheel systems are those of the group 6 transition metals and an analysis of bonding in these systems provides significant insight into their spectroscopic behavior. The bonding is easily understood by the fragment orbital method, whereby we consider the face-to-face interaction of two square planar fragments (see Figure 1.2 on next page). The metal-ligand bonds in the two fragments can be rationalized using a hybrid set of orbitals with the following atomic orbital basis: s, p_x, p_y, and $d_{x^2-y^2}$. The four remaining d-orbitals are then free to form the metal-metal bond. The metal-metal bonding in this case is resultant from three different modes of orbital overlap, namely σ, π, and δ orbital overlap. The σ bond is the strongest and results from the head-to-head overlap of the metal dz^2 orbitals. The next strongest bonding contribution arises from side-to-side orbital overlap of the degenerate d_{xz} and d_{yz} orbitals on the respective metals. This generates the MM π bonds. The weakest contribution is from the delta interaction, which arises from the face-to-face interaction of the d_{xy} orbital on the respective metal atoms.

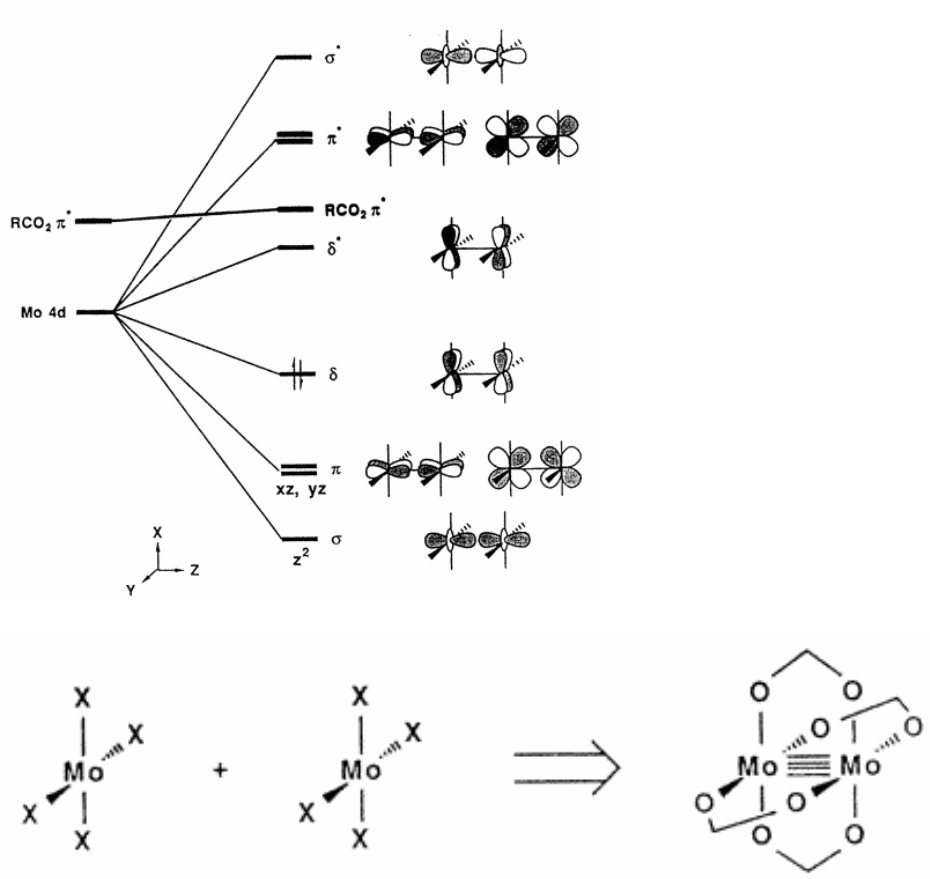

Figure 1.2 Frontier molecular orbital diagram for dimolybdenum tetracarboxylate paddle wheel complexes (Extract from Ref. 3).

1.5 Comparison of molybdenum versus tungsten

Furthermore, the energies of the resultant molecular orbitals depend largely upon the principle quantum number of the group 6 metal in question. Tungsten, which lays one row beneath molybdenum in the periodic table, has higher lying orbitals that more closely match the energies of the orbitals of interest on the carboxylate, namely the CO_2 π^* orbitals. This affects the magnitude of the orbital splitting and has important implications in the spectroscopic attributes of the respective systems.

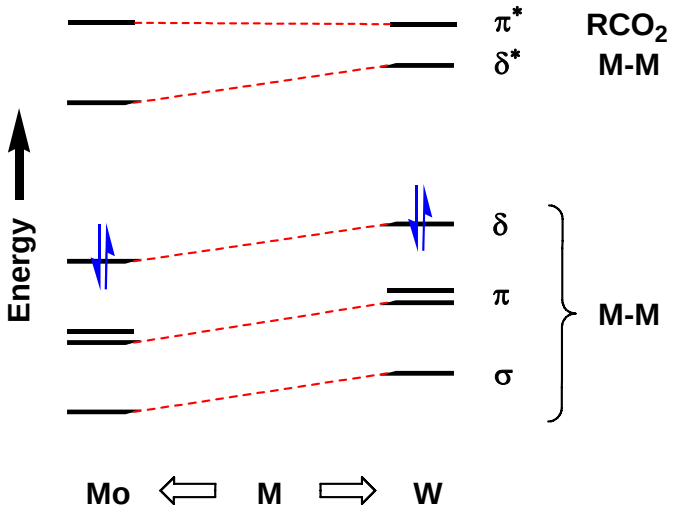

Figure 1.3 Frontier molecular orbital diagram for $M_2(O_2CR)_4$, M = Mo or W (Extracted from Ref. 6).

1.6 Electronic Absorptions

The dimetal paddlewheel complexes are often intensely colored due to strong electronic absorptions in the visible region of the electromagnetic spectrum. The disparity between electronic transitions in mononuclear and quadruply bonded paddlewheel complexes is markedly pronounced, with a new set of transitions consequential of the δ overlap. These dimetal paddlewheel complexes typically display three types of electronic transitions, namely the M_2-δ to M_2-δ* (d-d), M_2-δ to L- π * metal-to-ligand charge transfer (MLCT), and the L- π to L- π *. While the δ to δ* transition (metal-centered transition) is common, it is not often observed because of its low molecular absorptivity and tendency to coincide with or be obscured by more intense transitions. The most significant transition in these dimetal paddlewheel complexes is the MLCT transition, which is an intense transition and provides considerable insight into the

energy gap between the M_2 δ and CO_2 π * orbitals. As mentioned earlier, tungsten bears higher lying atomic orbitals, which more closely match the π * orbitals on the carboxylate (or other π* orbitals of bridging ancillary ligands), thus yielding lower energy MLCT transitions. The last type of transition is the L- π to L- π * and is similar in intensity to the MLCT band.

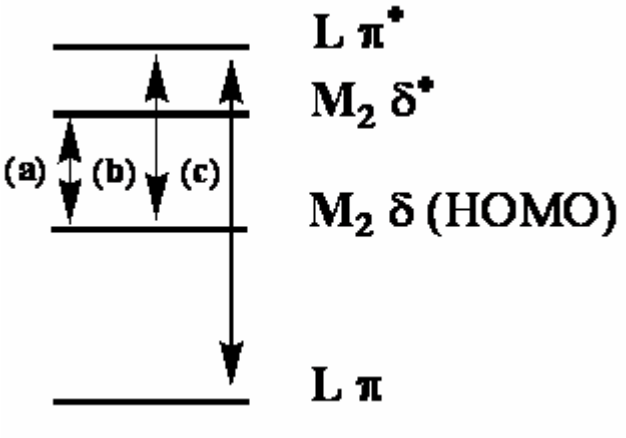

Figure 1.4 Schematic illustrating the typical electronic absorptions for dimetal paddlewheel complexes: (a) M_2 δ → M_2 δ^* transition (d-d), (b) M_2 δ → L π^* transition (MLCT), and (c) L π → L π^* transition.

1.7 Introductory comments on linked species

While simple dimers of paddlecomplexes are of significant interest to us, it is linked paddlewheel complexes that show the most promise for applicability in electronic devices. Chisholm and coworkers, with the successful linkage of paddlewheel complexes via unsaturated dicarboxylates, first introduced the concept of these so-called dimers of dimers in the late 1980's and early 1990's.[7] It was demonstrated that the dimetal centers in these dimers of dimers could electronically couple with one another, and thus, complexes of the form $[M_2(O_2CR)_3]$(μ-linker), as well as non-carboxylate analogs,

provide an ideal basis for the study of mixed-valence complexes. Oxidation of two linked M_2 units yields a mixed valence compound. A study of these complexes may help to demarcate the boundaries defining class 2 mixed-valence complexes in the Robin-Day classification scheme.

1.8 Mechanisms of electronic coupling in linked species

Linked dimetal paddlewheel complexes may electronically couple with each other through two possible mechanisms: (1) electrostatic interactions and (2) interaction between the M_2 δ orbitals with the π and the π* orbitals of the linker; the former interaction being a filled-filled interaction with the latter being a filled-empty interaction.[8] These orbital interactions yield two types of orbital combinations: (1) out-of-phase and (2) in-phase orbital combinations as defined with respect to the sign on the δ orbitals on the respective dimetal units.

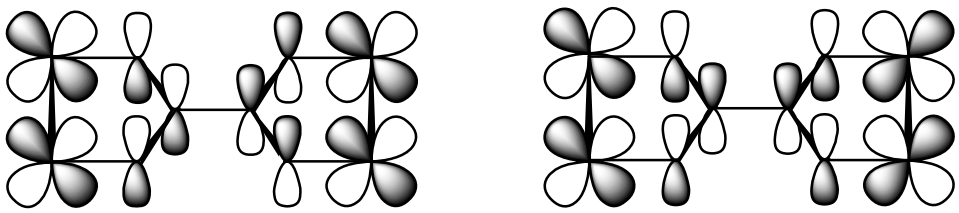

Figure 1.5 (A) out-of-phase δ orbital combination and (B) in-phase δ orbital combination showing the electronic coupling in oxalate bridged complexes (Extracted from Ref. 6).

1.9 Classification of mixed-valence compounds as per the Robin-Day method

Mixed valence complexes are categorized into one of three classes according to the Robin-Day classification scheme.[9] Class I complexes are those which exhibit

minimal or no electronic coupling between the respective metal units, and hence are viewed as valence trapped species. At the other extreme are Class III complexes, whereby the coupling is so significant that full delocaliztion is observed. Class II is thus the intermediate case, where neither valence trapped nor full delocalization is an appropriate description. Here there is a significant thermal energy barrier to electron transfer and the appearance of an electronic transition in the near IR corresponds to photoinduced electron transfer.

In the case where electron transfer is not resultant from electrostatic interactions and is attributable to metal-linker interaction, the coupling mechanism is coined superexchange.[10] Two types of superexchange must be considered: (1) electron transfer superexchange and (2) hole transfer superexchange.[10] In the former mechanism, the dominant component on the linker is the LUMO, or the empty π^* orbital. In the latter case, the dominant component on the linker is the HOMO, or the filled π orbital, whereby optical excitation from one minimum encourages the transfer of an electron from one metal to the other. In reality, the electronic coupling can be a culmination of one or both of these processes.

1.10 Quantization of electronic coupling

The magnitude of electronic coupling in mixed valence species is most easily estimated via electrochemical methods. This is accomplished by determining the separation between the first and second one-electron oxidation potentials [$E_{1/2}$(II) – $E_{1/2}$(I)].[11] The rational for this quantization is that after the 1st electron oxidation, several cases may be observed: (1) valence trapped behavior whereby there will be a positive

charge localized on one redox center, while the other will remain neutral (class I behavior), (2) partial delocalitzation whereby each redox center will bear some net positive charge (class II behavior), and (3) complete delocalization with a formal +1/2 charge residing on both redox centers (class III behavior). Each one of these cases will yield different magnitudes in potential separation, with little separation observed in the first case (<150 mV), moderate separation in the second case (150 to 350 mV), and large separation in the third case (>350 mV). The actual magnitude of $\Delta E_{1/2}$ is, however, dependent on the solvent and the counteranion which means that distinguishing between class II and III is not possible by electrochemical methods alone.

1.11 Discussion of metal-ligand interactions and implications on substitution chemistry.

Ligand-metal interactions in the paddlewheel complexes can be viewed as Lewis acid-base interactions, with the metals acting as Lewis acids by accepting electron density via donation from the ligands. Thus, it is a reasonable assumption that less basic ligands could be substituted by more basic ones; however steric interactions and relative solubility must be taken into consideration. Hence, the substitution chemistry of dimetal paddlewheel compounds is a culmination of both kinetic and thermodynamic attributes, which often are in competition with one another.

1.12 Synthesis of dimolybdenum tetracarboxylates

The dimolybdenum tetracarboxylates, $Mo_2(O_2CR)_4$, are easily prepared in near quantitative yield through the thermal reaction of $Mo(CO)_6$ with a carboxylic acid in a

high boiling point solvent, such as diglyme or *o*-dichlorobenzene.[12] Analogous reactions using $W(CO)_6$ fail to yield the corresponding ditungsten tetracarboxylates, $W_2(O_2CR)_4$, instead producing polymeric or high-oxidation-state tungsten trinuclear species.[13] It is only by a low yielding, tedious reaction that these ditungsten tetracarboxylates are produced.[14]

1.13 Synthesis and structure of ditungsten tetrakis(mhp)

In fact, very few ditungsten paddlewheel complexes can be prepared directly from $W(CO)_6$, with $W_2(mhp)_4$ being a rare exception, (mhp is the anion of 2-hydroxy-6-methylpyridine). $W_2(mhp)_4$ is easily prepared by the thermal reaction of $W(CO)_6$ with a stoichiometric amount of 2-hydroxy-6-methylpyridine in a high boiling point solvent.[15] The mhp ligand is asymmetric, unlike the carboxylates, and hence, in theory, $Mo_2(mhp)_4$ could exist as one of several isomers: (1) all mhp methyl groups pointing towards one axial site of the paddlewheel complex, (2) three mhp methyl groups pointing towards one axial site and the remaining one facing the other axial site, and (3) two mhp methyl groups pointing towards both of the respective axial sites on the paddlewheel complexes and for this arrangement there are also two possibilities. That stated, the complex is only known to exist as one of the possible isomers, with the face of the mhp ligand alternating around the paddlewheel complex (see Figure 3 on next page). This isomeric preference is likely favored by the minimization of steric repulsion between the methyl groups on the respective mhp ligands, as otherwise the trans influence would favor no facial alternation of the mhp ligand about the paddlewheel complex.

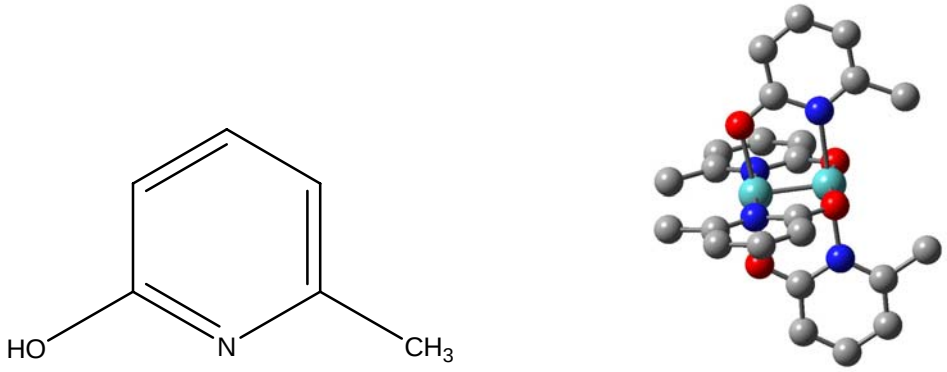

Figure 1.6 Left: free Hmhp ligand and Right: structure of $Mo_2(mhp)_4$.

1.14 Advantages of $M_2(mhp)_4$ systems

The advantages of using the anion of 2-hydroxy-6-methylpyridine (mhp) as an auxiliary ligand in dimetal paddlewheels are threefold: (1) the ligand should be noticeably less labile than carboxylates, (2) the nitrogen donor should render the mhp ligand as superior in magnitude with respect to the trans influenc of the carboxylates, and (3) the tungsten analog can be readily synthesized. The fact that the mhp ligand is less kinetically labile could afford geometry preservation in the synthesis of mixed-ligand species. Furthermore, the mhp ligands can serve as anchors, promoting site-specific synthesis in activated synthetic analogs, i.e. cationic derivatives. Lastly, the greater trans influence of the nitrogen donar should afford the synthesis of reactive cis-directing units for the synthesis of cyclic oligomers.

1.15 Basic synthetic strategies

The synthetic strategies used can be roughly divided into two classes: (1) simple ligand exchange reactions and (2) salt metathesis reactions using cationic species.

Ligand exchange reactions are the simpler of the two classes and may be applicable when equilibrium processes are anticipated to yield a desired product. Non-equilibrium chemistry may be observed when the desired product is exceedingly less soluble than the reactant and all other undesirable products. The other synthetic method, involving the use of cationic derivatives provide rigorous control over substitution patterns providing the product is not kinetically labile to ligand scrambling. That stated the use of cationic derivatives is currently limited to molybdenum systems.

CHAPTER 2

DEVELOPMENT OF ALTERNATE ROUTES INTO THE DITUNGSTEN TETRACARBOXYLATES

2.1 Introduction

The dimetal tetracarboxylates have historically been used as starting points for the synthesis of a wide variety of complexes containing the M_2^{4+} core, primarily because of the kinetic lability of the carboxylate ligand. The most exploited synthetic route for $Mo_2(O_2CR)_4$ complexes involves the thermal reaction of a carboxylic acid and $Mo(CO)_6$ in a high boiling solvent.[12]

Unfortunately, analogous reactions using $W(CO)_6$ do not afford the corresponding $W_2(O_2CR)_4$ complexes.[13] However, the ditungsten paddlewheel complexes, by virtue of their higher-lying orbitals, may prove to be more viable candidates than their molybdenum counterparts in electronic applications. It is in this light that we became interested in developing alternate synthetic routes for $W_2(O_2CR)_4$ complexes.

The reaction of $W(CO)_6$ and 2-hydroxy-6-methylpyridine (Hmhp) directly produces $W_2(mhp)_4$ (where mhp is the anion of Hmhp) in high yield.[15] The ease in preparation of $W_2(mhp)_4$ motivated us to investigate its substitution behavior with a variety of carboxylic acids including 2-thienylcarboxylic acid, benzoic acid, 9-anthracenylcarboxylic acid, and 2,4,6-triisopropylbenzoic acid.

2.2 Results and discussion

The reaction of $W_2(mhp)_4$ and RCO_2H, where R = 2-thienyl and Ph, yielded the mixture $W_2(mhp)_{4-x}(O_2CR)_x$ (x = 1-4). In the reaction where the concentration of RCO_2H was four orders of magnitude greater than the stoichiometric equivalent, the predominant species observed was $W_2(O_2CR)_4$. Thus, it can be concluded that for benzoic acid and 2-thienylcarboxylic acid, the starting material and desired product do not differ significantly in either thermodynamic stability or solubility, and hence, complexes of all orders of substitution coexist in equilibrium.

The reaction of $W_2(mhp)_4$ and Anth-9-CO_2H did not display the above equilibrium behavior and yielded $W_2(O_2C\text{-}9\text{-}Anth)_4$. This reaction is likely driven by differential solubility, whereby $W_2(mhp)_4$ is rather soluble in toluene at an elevated temperature, but $W_2(O_2C\text{-}9\text{-}Anth)_4$ is not. Thus, the ligand exchange reaction of $W_2(mhp)_4$ with Anth-9-CO_2H provides a convenient synthetic route for a $W_2(O_2CR)_4$ complex.

The reaction of $W_2(mhp)_4$ and TiPB yielded an intensely bright red colored complex, which was confirmed as $W_2(mhp)_2(TiPB)_2$. The ^{1}H-NMR spectrum indicated that the isopropyl groups on the TiPB ligand are not diastereotopic, and hence it can be argued that the TiPB ligands are trans to each other. Conversely, the cis-configuration has no mirror plane, and thus it would be expected for the isopropyl substituents on the TiPB ligand to be diastereotopic thereby rendering them distinguishable by ^{1}H-NMR spectroscopy.

2.3 Experimental Section

All experiments were conducted using standard glove box and Schlenk techniques. Solvents were dried and degassed prior to use by standard procedures. All reactions and subsequent workups were carried out under an argon environment. All reagents were used as received.

$W_2(mhp)_4$

$W_2(mhp)_4$ was prepared through the thermal reaction of $W(CO)_6$ and a stoichiometric amount of 2-hydroxy-6-methylpyridine, as per the literature preparation.[15]

Reaction of $W_2(mhp)_4$ and 2-thienylcarboxylic acid (th-2-CO_2H) (4 eq)

A Schlenk flask was charged with 0.128 g (1.0 mmol) of 2-thienylcarboxylic acid, 0.200 g (0.25 mmol) of $W_2(mhp)_4$, and 15 mL of toluene. The flask was placed in a 50 °C oil bath, and the reaction mixture was stirred gently. The solution turned from a red to a dark purple color, within minutes. The solution was allowed to stir in the oil bath for 3 days. After which, the reaction mixture was cooled to room temperature and the product was collected on a frit. The product was washed three times with toluene (15 mL total) and once with hexanes (5 mL), then dried under vacuum. The ^1H NMR spectrum was complex with multiple mulitplets appearing in the aromatic range (6.0 – 8.0 ppm), which was indicative of a mixture of products. MALDI-TOF: Calculated MW for $W_2C_{24}N_4O_4H_{23}$: 799.37 (M^+), calculated MW for $W_2C_{23}N_3O_5SH_{20}$: 818.32 (M^+), calculated MW for $W_2C_{22}N_2O_6S_2H_{17}$: 837.27 (M^+), calculated MW for $W_2C_{21}NO_6S_3H_{16}$:

842.25 (M^+), calculated MW for $W_2C_{20}O_8S_4H_{11}$: 875.17 (M^+): observed: 799.55, 818.49, 837.45, 856.41, and 875.36.

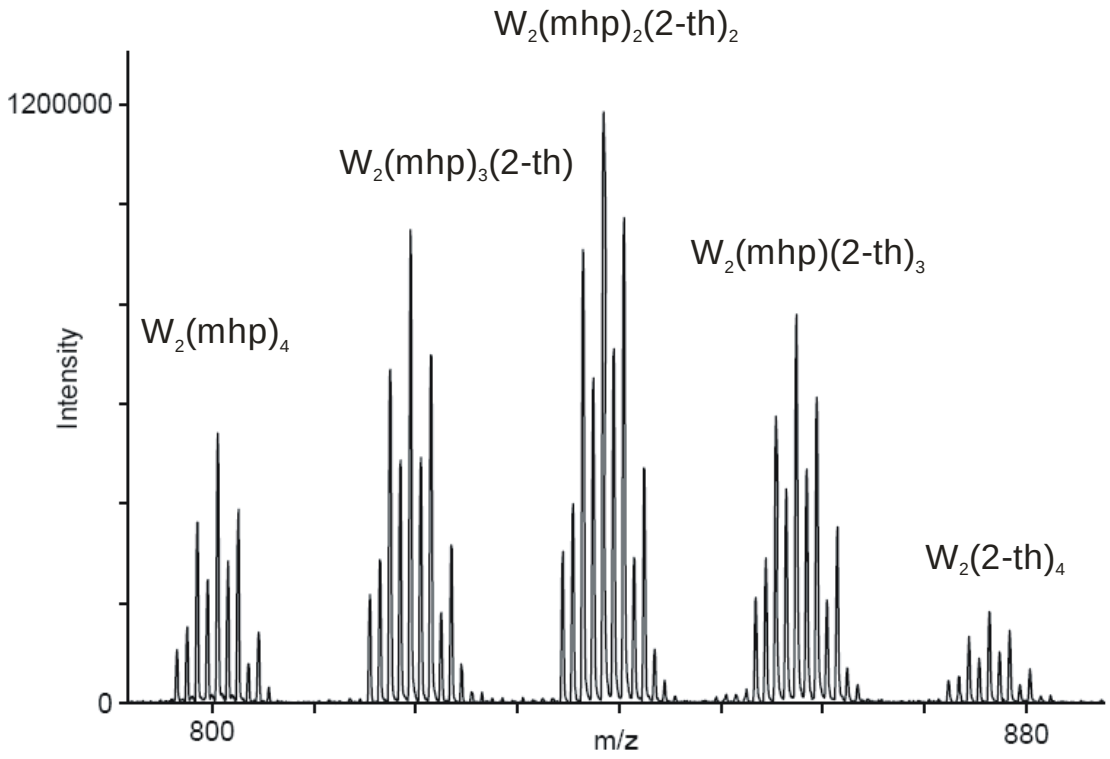

Figure 2.1 *MALDI spectrum for the product of the reaction of $W_2(mhp)_4$ and 4 2-thienylcarboxylic acid, where 2-th represents the anion of 2-thienylcarboxylic acid.*

Reaction of $W_2(mhp)_4$ and benzoic acid (Ph-CO_2H) (4 eq)

A Schlenk flask was charged with 0.153 g (1.25 mmol) of benzoic acid, 0.250 g (0.31 mmol) of $W_2(mhp)_4$, and 15 mL of toluene. The flask was placed in a 70 °C oil bath, and the reaction mixture was stirred gently for 24 h. The solution turned from a red to a dark purple color, within minutes. The solution was allowed to stir in the oil bath for 3 days. After which, the reaction mixture was cooled to room temperature and the solid product was collected on a frit. The product was washed once with toluene (10 mL) and three times with hexanes (15 mL), then dried under vacuum. The ^{1}H NMR spectrum was

complex with multiple mulitplets appearing in the aromatic range (6.0 – 8.0 ppm), which was indicative of a mixture of products. MALDI-TOF: Calculated MW for $W_2C_{24}N_4O_4H_{23}$: 799.37 (M^+), calculated MW for $W_2C_{25}N_3O_5H_{22}$: 812.3 (M^+), calculated MW for $W_2C_{26}N_2O_6H_{21}$: 825.23 (M^+), calculated MW for $W_2C_{27}NO_7H_{20}$: 838.16 (M^+), calculated MW for $W_2C_{28}O_8H_{19}$: 851.09 (M^+), observed: 799.85, 812.84, 825.84, 838.82, and 821.81.

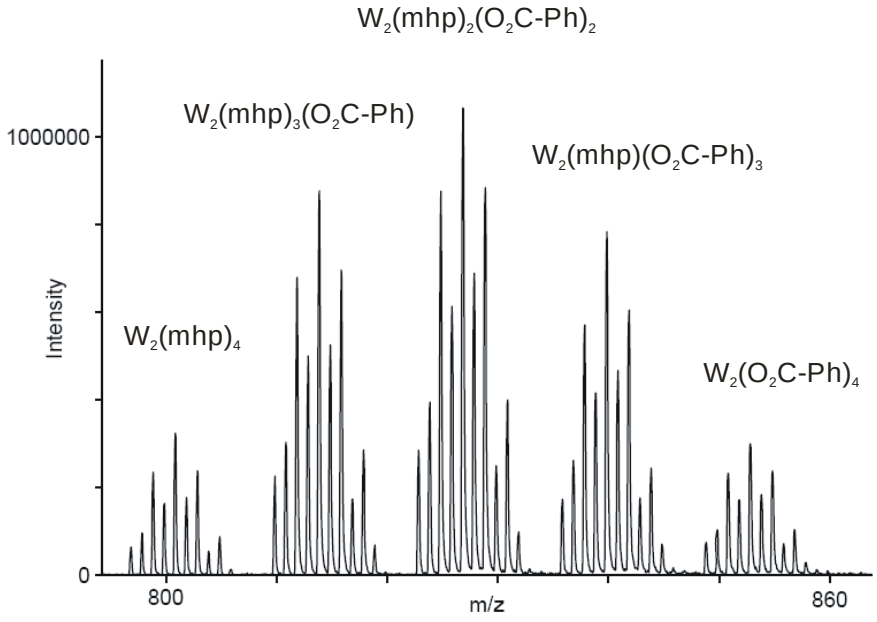

Figure 2.2 *MALDI spectrum for the product of the reaction of $W_2(mhp)_4$ and 4 Ph-CO_2H.*

Reaction of $W_2(mhp)_4$ and benzoic acid (Ph-CO_2H) (8 eq)

A Schlenk flask was charged with 0.244 g (1.99 mmol) of benzoic acid, 0.200 g (0.25 mmol) of $W_2(mhp)_4$, and 15 mL of toluene. The flask was placed in a 60 °C oil bath, and the reaction mixture was stirred gently for 24 h. The solution turned from a red to a dark purple color, within minutes. The solution was allowed to stir in the oil bath for 3 days. After which, the reaction mixture was cooled to room temperature and the solid product

was collected on a frit. The product was washed once with toluene (10 mL) and three times with hexanes (15 mL), then dried under vacuum. The ^{1}H NMR spectrum was complex with multiple mulitplets appearing in the aromatic range (6.0 – 8.0 ppm), which was indicative of a mixture of products. MALDI-TOF: Calculated MW for $W_2C_{24}N_4O_4H_{23}$: 799.37 (M^+), calculated MW for $W_2C_{25}N_3O_5H_{22}$: 812.3 (M^+), calculated MW for $W_2C_{26}N_2O_6H_{21}$: 825.23 (M^+), calculated MW for $W_2C_{27}NO_7H_{20}$: 838.16 (M^+), calculated MW for $W_2C_{28}O_8H_{19}$: 851.09 (M^+), observed: 799.62, 812.60, 825.58, 838.58, and 851.61.

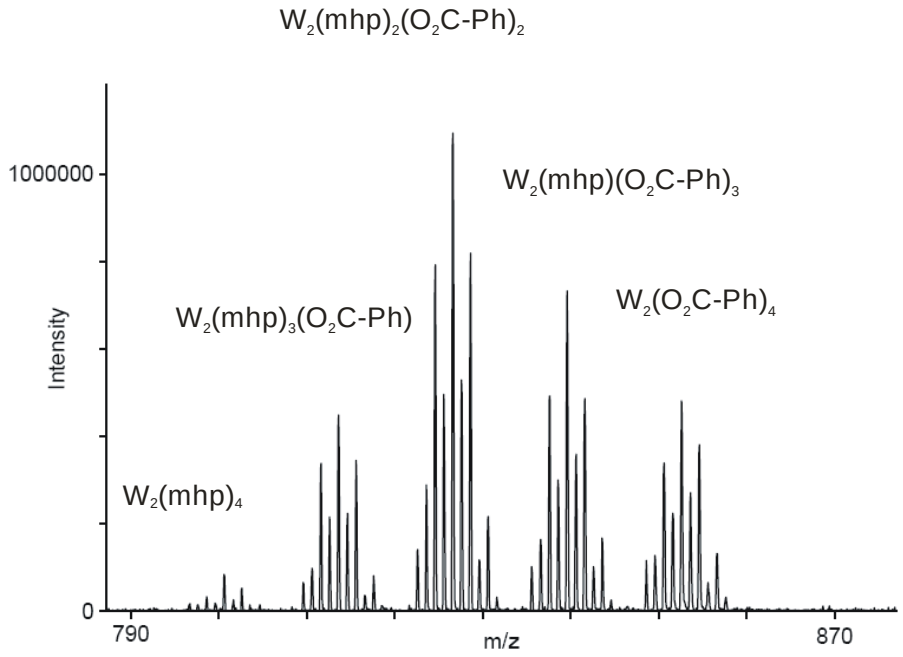

Figure 2.3 *MALDI spectrum for the product of the reaction of $W_2(mhp)_4$ and 8 Ph-CO_2H.*

Reaction of $W_2(mhp)_4$ and benzoic acid (Ph-CO_2H) (16 eq)

A Schlenk flask was charged with 2.345 g (19.2 mmol) of benzoic acid, 1.000 g (1.25 mmol) of $W_2(mhp)_4$, and 50 mL of toluene. The flask was placed in a 60 °C oil bath, and

the reaction mixture was stirred gently for 16 h. The solution turned from a red to a dark purple color, within minutes. The solution was allowed to stir in the oil bath for 3 days. After which, the reaction mixture was cooled to room temperature and the solid product was collected on a frit. The product was washed once with toluene (10 mL) and three times with hexanes (15 mL), then dried under vacuum. The ^{1}H-NMR spectrum displayed similar behavior to those above, but the corresponding peaks for coordinated benzoate were much more intense than before. MALDI-TOF: Calculated MW for $W_2C_{24}N_4O_4H_{23}$: 799.37 (M^+), calculated MW for $W_2C_{25}N_3O_5H_{22}$: 812.3 (M^+), calculated MW for $W_2C_{26}N_2O_6H_{21}$: 825.23 (M^+), calculated MW for $W_2C_{27}NO_7H_{20}$: 838.16 (M^+), calculated MW for $W_2C_{28}O_8H_{19}$: 851.09 (M^+), observed: 812.67, 825.68, 838.69, and 851.70.

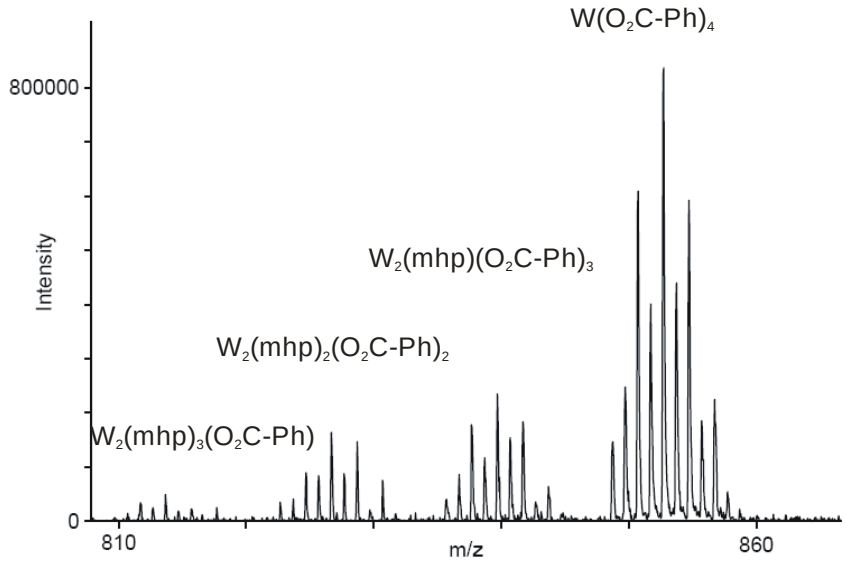

Figure 2.4 *MALDI spectrum for the product of the reaction of $W_2(mhp)_4$ and 16 Ph-CO_2H.*

Reaction of $W_2(mhp)_4$ and 9-anthracenylcarboxylic acid (Anth-9-CO_2H)

A Schlenk flask was charged with 0.278 g (1.25 mmol) of Anth-9-CO_2H, 0.250 g (0.31 mmol) of $W_2(mhp)_4$, and 15 mL of toluene. The flask was placed in a 60 °C oil bath, and the reaction mixture was stirred gently for 16 h. The solution turned from a red to a dark purple color, within minutes. The solution was allowed to stir in the oil bath for 3 days. After which, the reaction mixture was cooled to room temperature and the solid product was collected on a frit. The product was washed three times with toluene (15 mL total), once with DMSO (5 mL), and three times with hexanes (15 mL), and then dried under vacuum. 0.220 g of product was recovered (66% yield). ^{1}H NMR (DMSO, δ, ppm): 6.92, 6.95, 6.95 (t), 7.28, 7.29, 7.32 (t), 7.96, 7.99 (d), 8.43 (s), 8.47, 8.50 (d). MALDI-TOF: Calculated MW for $W_2C_{60}O_8H_{36}$: 1251.57 (M^+), observed 1252.2.

Reaction of $W_2(mhp)_4$ and 2,4,6-triisopropylbenzoic acid (TiPB) to yield $W_2(mhp)_2(TiPB)_2$

A Schlenk flask was charged with 0.248 g (1.0 mmol) of TiPB, 0.200 g (0.25 mmol) of $W_2(mhp)_4$, and 10 mL of toluene. The flask was placed in a 45 °C oil bath, and the reaction mixture was stirred gently for 16 h. The solution turned from a red to an intensely bright red color, within minutes. The solution was allowed to stir in the oil bath for 3 days. After which, the reaction mixture was cooled to room temperature and the solid product was collected on a frit. The product was washed three times with hexanes (15 mL), then dried under vacuum. 0.143 g of product was recovered (42 % yield). ^{1}H NMR (DMSO, δ, ppm): 0.99, 1.02 (d, CH_3 of TiPB), 1.19, 1.22 (d, CH_3 of TiPB), 2.22 (s, CH_3 of mhp), 2.45-2.58 (m, CH of TiPB), 2.77-2.89 (m, CH of TiPB), 6.46, 6.47, 6.49

(t, CH of mhp), 6.95 (s, CH of TiPB), 7.08-7.10 (m, CH of mhp). MALDI-TOF: Calculated MW for $W_2C_{44}O_6N_2H_{57}$: 1077.44 (M^+), observed 1077.1.

CHAPTER 3

THE ELECTRONIC MODIFICATION OF DIMOLYBDENUM AND DITUNGSTEN PADDLEWHEEL COMPLEXES

3.1 Introduction

Dimetal paddlewheel complexes typically display three types of electronic transitions, namely the M_2-δ to M_2-δ* (d-d), M_2-δ to L- π * metal-to-ligand charge transfer (MLCT), and the L- π to L- π *. Clearly, the energy of the MLCT electronic transition depends upon the relative energy of the metal-centered δ manifold with respect to the π -system of the ligand. Thus, the spectroscopic properties can be tuned by the proper choice and/or combination of ancillary ligands. Furthermore, the oxidative properties of the dinuclear center can be tuned through raising and lowering the metal orbital manifold through the selective choice of ancillary ligands.

With our discovery of the $W_2(mhp)_2(TiPB)_2$ complex, we became curious as to how the dimetal center (M = Mo or W) and nature of the ancillary ligands would modify the electronic properties of these dimers. The first comparison to be made was that amongst the mixed-ligand ditungsten complex with its molybdenum analogue. Next, we devised a plan to complete the series of complexes represented by $Mo_2(mhp)_{4-x}(TiPB)_x$ (where x = 1-4).

3.2 Results and discussions

The partial substitution of mhp ligands by TiPB ligands yielded the mixed-ligand $Mo_2(mhp)_2(TiPB)_2$ species, while $Mo_2(mhp)_3(TiPB)$ was produced through a salt metathesis reaction. The synthesis of $Mo_2(mhp)(TiPB)_3$ is currently in progress.

3.2.1 UV–vis and electrochemical studies

The $M_2(mhp)_2(TiPB)_2$ complexes, where M = Mo and W, were analyzed via UV–vis spectroscopy.

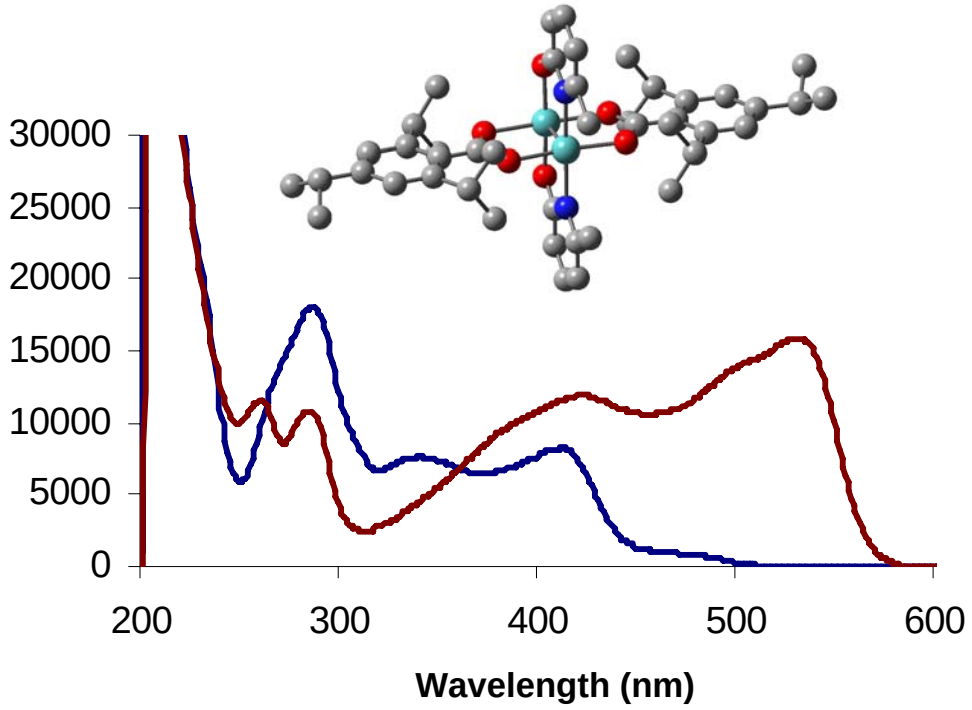

Figure 3.1 UV–vis spectra of $M_2(mhp)_2(TiPB)_2$ [M=Mo (blue); M=W (red)] complexes in THF at room temperature.

Tungsten has higher-lying orbitals, which more closely match the energies of the π* orbitals of the ancillary ligands, and hence the metal-ligand electronic transitions, namely

the MLCT bands, for $W_2(mhp)_2(TiPB)_2$ are significantly red-shifted with respect to the molybdenum analogue (See Figure 3.1 on previous page). As should be expected, the π to π* electronic transitions occurred at identical wavelengths for both molybdenum and tungsten. For both $Mo_2(mhp)_2(TiPB)_2$ and $W_2(mhp)_2(TiPB)_2$ two MLCT bands are observed, one TiPB based and one mhp based. Although, the respective transitions cannot be assigned with absolute certainty in the absence of theoretical calculations, predictions can be made when compared with the $M_2(mhp)_4$ and $M_2(TiPB)_4$ spectra, shown in Figure 3.2 for molybdenum (below).

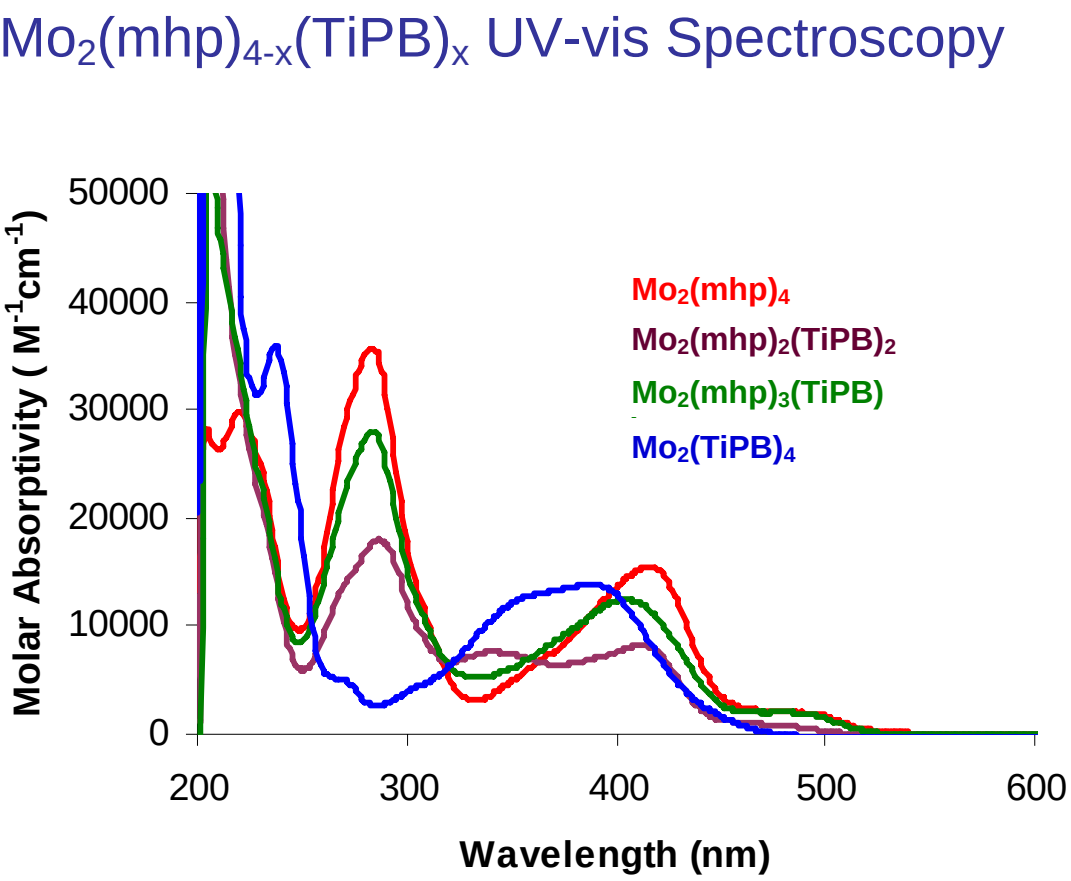

Figure 3.2 UV-vis for the $Mo_2(mhp)_{4-x}(TiPB)_x$ (where x = 0, 1, 2, and 4)

The UV-vis spectrum of $Mo_2(mhp)_4$ displays a MLCT band at around 430 nm. In addition to this MLCT in the UV-Vis spectrum of $Mo_2(mhp)_2(TiPB)_2$, which occurs with a lower molecular absorptivity with respect to that for $Mo_2(mhp)_4$, a second MLCT band is observed at higher energy. Thus, it can be concluded that the MLCT band observed around 430 nm is mhp-based and that the higher energy MLCT band is TiPB-based. While not confirmed for the tungsten analogue, no reversal of the respective MLCT bands is expected. We therefore propose that the absorptions at 550 and 420 nm for $W_2(mhp)_2(TiPB)_2$ in Figure 3.1 arise from MLCT transitions to the mhp and TiPB ligands, respectively.

Another interesting feature displayed by the above spectra, is that the ligand-centered transition, LLCT, occurring slightly below 300 nm, decreases in intensity as the mhp ligands are substituted for TiPB ligands, and in the limit of reaching the homoleptic TiPB complex, no absorption is observed at 290 nm. Thus, through stepwise ligand substitution it was demonstrated that the absorption properties of dimolybdenum paddlewheel complexes could be controlled across a region spanning nearly 150 nm.

3.3 Experimental Section

All experiments were conducted using standard glove box and Schlenk techniques. Solvents were dried and degassed prior to use. All reactions and subsequent workups were carried out under an argon environment. All reagents were used as received.

$Mo_2(mhp)_4$

$Mo_2(mhp)_4$ was prepared through the thermal reaction of $Mo(CO)_6$ and a stoichiometric amount of 2-hydroxy-6-methylpyridine, as per the literature preparation.[15] This is identical to the preparation of tungsten analogue mentioned in the previous section.

$Mo_2(mhp)_2(TiPB)_2$

A Schlenk flask was charged with 0.395 g of TiPB (1.59 mmol, F.W. = 248.36 g/mol), 0.250 g of $Mo_2(mhp)_4$ (0.4 mmol, F.W. = 624 g/mol), and 10 mL of toluene. The flask was placed in a 60 °C oil bath, and the reaction mixture was stirred for 24 h. The solution turned from a rusty orange color to a bright yellow color within a half hour at 60 °C. After 24 h at elevated temperature, the reaction mixture was cooled to room temperature and the solid product was collected on a frit. The product was washed three times with hexane (15 mL total), then dried under vacuum. 0.294 g of a bright yellow powder was recovered (62% yield). ^{1}H NMR (DMSO, δ, ppm): 0.90, 0.92 (d, CH_3 of TiPB), 1.16, 1.18 (d, CH_3 of TiPB), 1.59 (s, CH_3 on mhp), 2.53-2.60 (m, CH of TiPB), 2.76-3.90 (m, CH of mhp), 6.55, 6.57 (d, H of mhp), 6.96 (s, H of TiPB), 7.05, 7.08 (d, H of mhp), 7.55, 7.58, 7.62 (t, H of mhp). MALDI-TOF: Calculated MW for $Mo_2C_{44}N_2O_6H_{58}$, 901.83 (M^+); found 902.13.

$[Mo_2(mhp)_3(CH_3CN)_2][BF_4]$

The $[Mo_2(mhp)_3(CH_3CN)_2]^+$ cation was prepared as per the literature.[16]

[$^{n}Bu_4N$][2,4,6-triisopropylbenzoate]

To a solution of 0.500 g of 2,4,6-triisopropylbenzoic acid (approximately 2 mmol, F.W. = 248.36 g/mol) in 5 mL of methanol was added 2.0 mL of a 1 M solution of n-butylammonium hydroxide in methanol. The mixture was stirred at room temperature for 1 hr and then stripped to dryness under vacuum at 50 °C.

$Mo_2(mhp)_3(TiPB)$

A solution of 0.200 g of $[Mo_2(mhp)_3(CH_3CN)_2][BF_4]$ (2.9 mmol, F.W. = 686.65 g/mol) in 15 mL of acetonitrile was combined with 0.143 g (2.9 mmol, F.W. = 490.36 g/mol) of [$^{n}Bu_4N$][2,4,6-triisopropylbenzoate] in a 10 mL solution of acetonitrile. Upon addition, a precipitate immediately formed and was collected on a frit. The product was washed three times with acetonitrile (15 mL total) and once with hexanes (5 mL), then dried under vacuum. ^{1}H NMR (DMSO, δ, ppm): 0.92, 0.95 (d, CH_3 of TiPB), 1.19, 1.22 (d, CH_3 of TiPB), 2.30 (s, CH_3 of mhp), 2.34 (s, CH_3 of mhp), 2.46-2.57 (m, CH of TiPB), 2.78-2.86 (m, CH of TiPB), 6.34, 6.37 (d, CH of mhp), 6.40, 6.43 (d, CH of mhp), 6.76, 6.79 (d, CH of mhp), 6.88, 6.92 (d, CH of mhp), 6.91 (s, CH of TiPB), 7.07-7.18 (m, CH of mhp), 7.23 (m, CH of mhp), 7.26-7.27 (m, CH of mhp). MALDI-TOF: Calculated MW for $Mo_2C_{34}O_5N_3H_{40}$, 762.57 (M^+); found 763.03

$Mo_2(mhp)(TiPB)_3$ [pending]

$Mo_2(mhp)(TiPB)_3$ will likely have to be accessed through the salt metathesis of $[Mo_2(TiPB)_3(CH_3CN)_2][BF_4]$ with a tetraalkylammonium salt of the mhp anion.

$[Mo_2(TiPB)_3(CH_3CN)_2][BF_4]$ is not a known complex and I am currently in the process of synthesizing it.

CHAPTER 4

SYNTHESIS AND CHARACTERIZATION OF DIMERS OF DIMERS

4.1 Introduction

Previously, it has been shown that paddlewheel complexes can be linked by a variety of dicarboxylate linkers of the form O_2C-X-CO_2, where x is an unsaturated backbone.[17] These dimers of dimers display unique electrochemical behaviors in that the dimetal centers can electronically couple with one another. This electronic coupling largely results from the interaction of the M_2-δ orbitals with the π and the π * orbitals of the linker.[18] We proposed the linkage of Mo_2 dimers by 2,5-thienyldicarboxylate, [2,5-th-$(CO_2)_2$)]$^{2-}$, and 3,4-thienyldicarboxylate, [3,4-th-$(CO_2)_2$]$^{2-}$, in order to ascertain how the geometry of the unsaturated linker affects the electronic coupling.

As previously mentioned, electrochemical methods are a basis by which the electronic coupling between dimetal centers can be gauged. In the electrochemical studies, the separation in potential between the 1st and 2nd one-electron oxidations provides a quantitative measure of the electronic coupling.[19] In this oxidative process, there are two limiting extremes: (A) valence trapped (class I behavior) and (B) full delocalization (class III behavior).[19] In the former case, the 1st and 2nd one-electron oxidations should occur at nearly identical potentials.[14] In the latter case, after the first electron is removed, a net ½ positive charge resides on both dimetal centers and thus the 2nd one-electron oxidation will occur at a much higher potential.[14]

4.2 Results and Discussions

$[Mo_2]_2$ dimers of dimers connected by unsaturated dicarboxylates can be produced through salt metathesis reactions. Simplified structures for the isomeric set of dimers of dimers that were synthesized are shown below in figures 4.1 and 4.2.

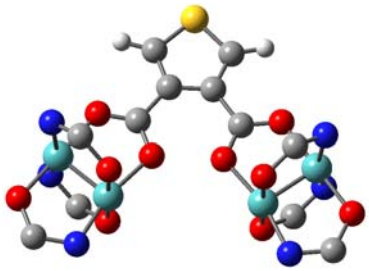

Figure 4.1 Proposed structure (simplified) of the $[(mhp)_3Mo_2]_2\{\mu\text{-}3,4\text{-}th\text{-}(CO_2)_2\}$ dimer of dimers.

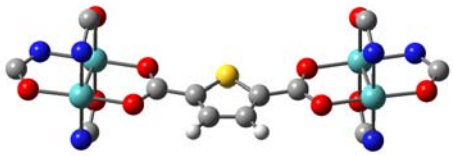

Figure 4.2 Proposed structure (simplified) of the $[(mhp)_3Mo_2]_2\{\mu\text{-}2,5\text{-}th\text{-}(CO_2)_2\}$ dimer of dimers.

The 1st and 2nd one-electron oxidations of the $[(mhp)_3Mo_2]_2\{\mu\text{-}3,4\text{-}th\text{-}(CO_2)_2\}$ dimer of dimers were separated by approximately 200 mV (see Figure 4.3 on next page). Unfortunately, the $[(mhp)_3Mo_2]_2\{\mu\text{-}2,5\text{-}th\text{-}(CO_2)_2\}$ dimer of dimers has defied current attempts in electrochemical studies. The electrochemical probe currently set up is strictly

for THF, in which $[(mhp)_3Mo_2]_2\{\mu\text{-}2,5\text{-}th\text{-}(CO_2)_2\}$ is insoluble. This problem should be rectified through the use of a DMSO electrolyte solution.

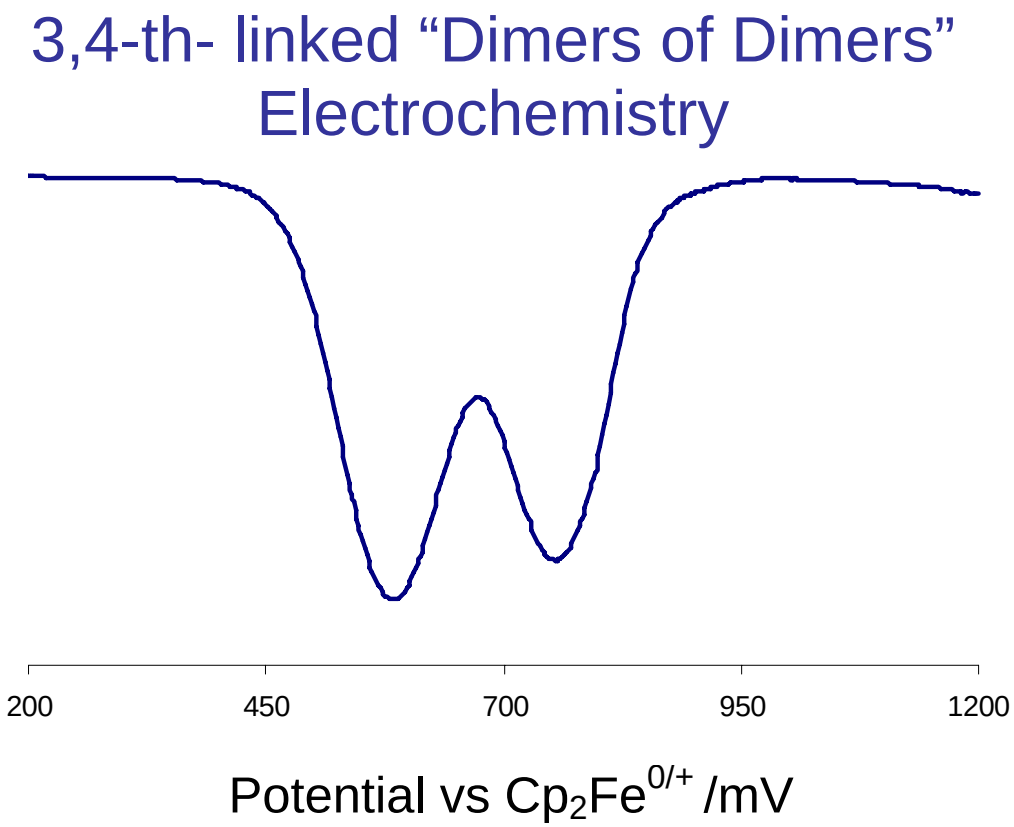

Figure 4.3 Differential pulse voltammogram for $[(mhp)_3Mo_2](\mu\text{-}3,4\text{-}th\text{-}(CO_2)_2)$.

The $[(mhp)_3Mo_2]_2\{\mu\text{-}2,5\text{-}th\text{-}(CO_2)_2\}$ dimer of dimers displayed a pronounced low energy MLCT band that most likely corresponds to the metal-to-linker charge transfer, while the corresponding band was much less apparent for the isomeric species, $[(mhp)_3Mo_2]_2\{\mu\text{-}3,4\text{-}th\text{-}(CO_2)_2\}$ (See Figure 4.4 on next page).

$[Mo]_4$ Dimers UV-vis spectroscopy

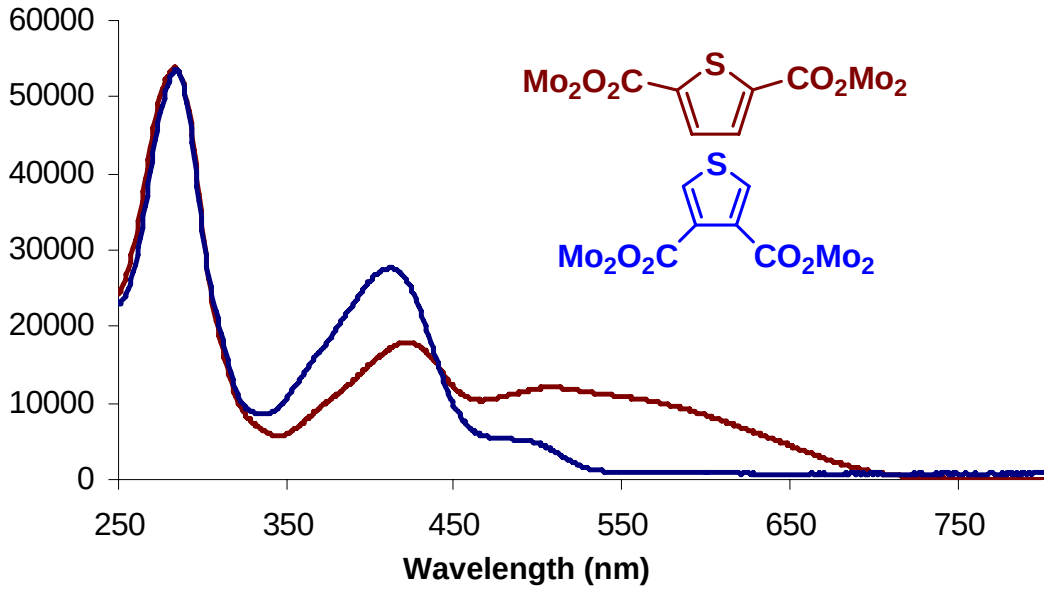

Figure 4.4 UV–vis spectra of the $[(mhp)_3Mo_2]_2\{\mu\text{-}2,5\text{-}th\text{-}(CO_2)_2\}$ [red] and $[(mhp)_3Mo_2]_2\{\mu\text{-}3,4\text{-}th\text{-}(CO_2)_2\}$ [blue] dimers of dimers at room temperature in THF solutions.

The linkage by 3,4-thienyldicarboxylate may bring the dimetal centers sufficiently close in proximity to one another that steric interactions arise (See figure 4.1 on the previous page). These energetically unfavorable interactions could be relieved by the twist of one dimetal center in relation to the other. As a consequence, the M_2-δ orbitals would have non-planar components with respect to the π -system of the linker. This is consistent with the absence of a low energy metal-to-linker charge transfer band in the UV–vis spectrum of $[(mhp)_3Mo_2]_2\{\mu\text{-}3,4\text{-}th\text{-}(CO_2)_2\}$. However, the observed electronic communication in

the E-chem could still result from electrostatic interactions even in the limit that the M_2-δ orbitals and the π -system of the linker lie completely orthogonal to each other.

The linkage by 2,5-thienyldicarboxylate should not introduce such steric interactions (See Figure 3) and the dimetal centers may prefer to be nearly coplanar with the linker in order to optimize backbonding with the π* orbitals. This would afford optimal overlap between the M_2-δ orbitals with the π -system of the linker, which is in accord with the observed low energy MLCT band in the UV–vis spectrum of $[(mhp)_3Mo_2]_2\{\mu\text{-}2,5\text{-}th\text{-}(CO_2)_2\}$.

4.3 Experimental section

All experiments were conducted using standard glove box and Schlenk techniques. Solvents were dried and degassed prior to use. All reactions and subsequent workups were carried out under an argon environment. All reagents were used as received.

$[Mo_2(mhp)_3(CH_3CN)_2][BF_4]$

The $[Mo_2(mhp)_3(CH_3CN)_2]^+$ cation was prepared as per the literature.[16]

$[^nBu_4N]_2[3,4\text{-}th(CO_2)_2]$

To a solution containing 0.028 g of 3,4-thienyldicarboxylic acid in 10 mL of methanol was added 0.320 mL of a 1 M solution of n-butylammonium hydroxide in methanol. The solution was stirred at room temperature for 1 hr and then stripped to dryness at 50 °C under vacuum.

[^{n}Bu$_4$N]$_2$[2,5-th(CO$_2$)$_2$]

To a solution containing 0.037 g of 2,5-thienyldicarboxylic acid in 5 mL of methanol was added 0.43 mL of a 1 M solution of n-butylammonium hydroxide in methanol. The solution was stirred at room temperature for 1 hr and then stripped to dryness at 50 °C under vacuum.

[(mhp)$_3$Mo$_2$]$_2${μ-3,4-th-(CO$_2$)$_2$}

A solution of 0.32 mmol of [Mo$_2$(mhp)$_3$(CH$_3$CN)$_2$][BF$_4$] in 20 mL of acetonitrile was combined with a solution of 0.16 mmol of [^{n}Bu$_4$N]$_2$[3,4-th(CO$_2$)$_2$] in 10 mL of acetonitrile. A precipitate formed and was collected on a frit. The product was washed three times with acetonitrile (15 mL total) and once with hexanes (5 mL), then dried under vacuum. ^{1}H NMR (DMSO, δ, ppm): 1.65 (s, CH$_3$ of mhp), 1.76 (s, CH$_3$ of mhp), 6.45, 6.48 (d, CH of mhp), 6.56, 6.59 (d, CH of mhp), 6.78-6.83 (m, CH of mhp), 7.35-7.51 (m, CH of mhp), 8.06, 8.07 (d, CH of thiophene). MALDI-TOF: Calculated MW for Mo$_4$C$_{42}$N$_6$O$_{10}$SH$_{37,}$ 1201.64 (M$^+$), observed 1201.6.

[(mhp)$_3$Mo$_2$]$_2${μ-2,5-th-(CO$_2$)$_2$}

A solution of 0.36 mmol of [Mo$_2$(mhp)$_3$(CH$_3$CN)$_2$][BF$_4$] in 20 mL of acetonitrile was combined with a solution of 0.18 mmol of [^{n}Bu$_4$N]$_2$[2,5-th(CO$_2$)$_2$] in 10 mL acetonitrile. A precipitate formed and was collected on a frit. The product was washed three times with acetonitrile (15 mL total) and once with hexanes (5 mL), then dried under vacuum.

^{1}H NMR (DMSO, δ, ppm): 1.66 (s, CH_3 of mhp), 1.82 (s, CH_3 of mhp), 6.41, 6.42 (d, H of mhp), 6.50, 6.52 (d, H of mhp), 6.74, 6.76 (d, H of mhp), 6.85, 6.87 (d, H of mhp), 7.16, 7.18 (d, H of mhp), 7.23, 7.24 (d, H of mhp), 7.33, 7.35 (d, H of mhp), 7.40, 7.42, 7.44 (t, H of mhp), 7.64 (s, H of thiophene). MALDI-TOF: Calculated MW for $Mo_4C_{42}N_6O_{10}SH_{37,}$ 1201.64 (M^+), observed 1202.8.

CHAPTER 5

ATTEMPTED SYSNTHESIS OF HIGHER-ORDER OLIGOMERS

5.1 Introduction

The concept of electronic coupling in higher-order oligomers, including molecular triangles and squares, is a topic of great interest to us. After the first electron oxidation of a $[M_2]_4$ molecular square, an unpaired electron could in principle be delocalized across 2 to 8 metal atoms. A study of the electronic behavior in mixed-valence molecular squares will serve as a benchmark, to which inferences can be derived pertaining to the electronic behavior in extended grid lattices of M_2^{4+} units.

The proper choice of both building block and linker is crucial to the proliferation of molecular triangles and squares. The building blocks must be able to influence the geometry throughout the process of self-assembly, which must be reinforced by the nature of the linker.

Our current strategy involves metathetic reactions of cis-$L_2M_2^{2+}$ salts with unsaturated dicarboxylate salts. To avoid undesirable polymerization, the self assembly of supramolecular structures via salt metathesis must be conducted in extremely dilute solutions. We have recently synthesized $[Mo_2(mhp)_2(CH_3CN)_4][BF_4]_2$, and the crystal structure demonstrates that the mhp ligands are cis to one another (See figure 5.1 on next

page).[20] This building block can be viewed as a cis-geometry enforcer with weakly coordinated acetonitrile molecules forming a reactive corner-piece.

The cis arrangement of the mhp ligands of the dication was rather predictable, as the acetonitrile molecules have a rather weak trans influence, and hence would prefer to be trans to stronger trans influencing ligands. That stated, there was one structural peculiarity that was not expected, namely the facial orientation of the mhp ligands. Previously, it was noted that the mhp ligands of $Mo_2(mhp)_4$ alternate in face about the paddlewheel. However, in the dicationic species the remaining mhp ligands have rearranged such that both the methyl groups on the respective ligands point toward the same axial coordination site, i.e. no facial alternation.

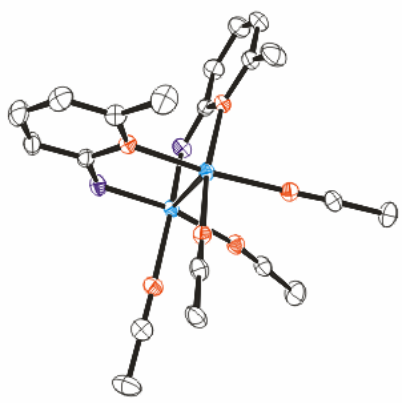

Figure 5.1 Crystal structure of $Mo_2(mhp)_2(CH_3CN)_4^{2+}$

5.2 Results and discussions

Through MALDI-TOF spectrometry it was determined that the reaction of $[Mo_2(mhp)_2(CH_3CN)_4][BF_4]_2$ and $[^nBu_4N]_2[O_2CC_6F_4CO_2]_2$ yielded a mixture of higher-order species including dimers of dimers, molecular triangles, and molecular squares (see

figure 5.2 below). The observed formation of the dimer of dimers is likely resultant from residual contamination of the dicationic sample with $[Mo_2(mhp)_3(CH_3CN)_2][BF_4]$. More interestingly is the formation of the cyclic-oligomers, namely the molecular triangles and squares. While the formation of one discrete cyclic-oligomer is ideal, the formation of both molecular triangles and squares can be rationalized by considering both kinetic and thermodynamic factors. The formation of molecular triangles requires the assembly of three dimetal units, and hence is kinetically favored. Furthermore, it should be expected that molecular triangle formation be entropically favored with respect to the formation of molecular squares. That stated, the angle strain in the molecular triangles should render the formation of this species unfavorable with respect to thermodynamics.

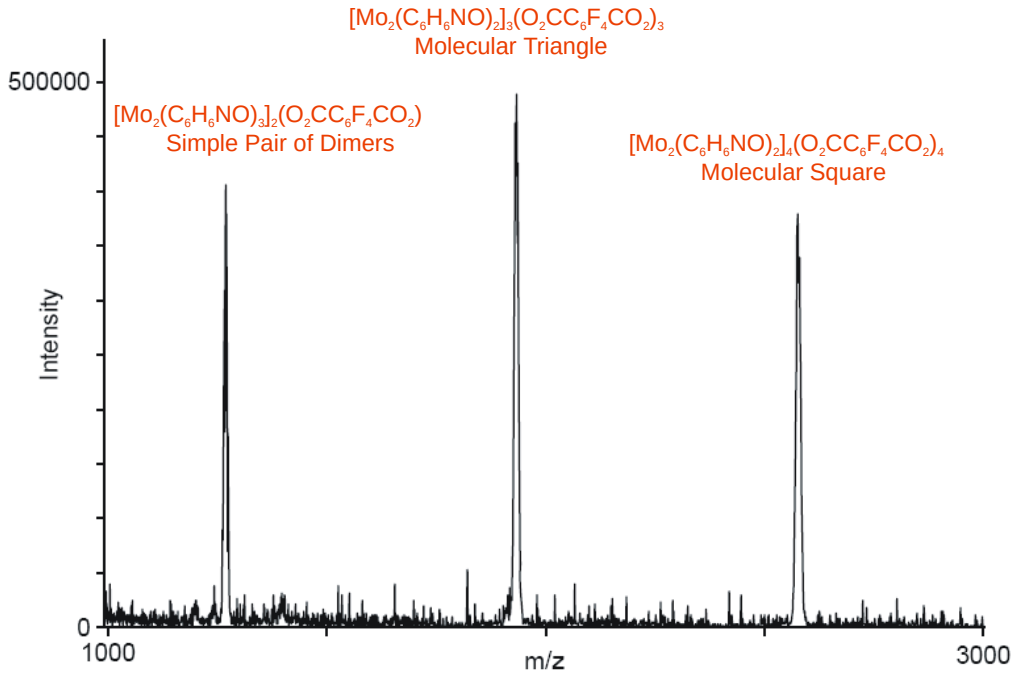

Figure 5.2 MALDI-TOF spectrum of resultant mixture.

We are currently interested in investigating the selective formation of molecular triangles and squares through the proper choice of linker. The use of short and rigid linkers will likely force the formation of molecular squares. On the other hand, the sole production of molecular triangles may be possible with the use of a bent linker. To that end, a variety of bent linkers will be employed in order to determine the optimal bend angle for the formation of molecular triangles. Molecular triangles may be favored in the case where the linker is slightly bent, 2,5-thienyldicarboxylate may prove to be particularly useful in this regard. The formation of molecular squares should be favored by short, rigid linkers like oxalate.

5.3 Experimental

All experiments were conducted using standard glove box and Schlenk techniques. Solvents were dried and degassed prior to use. All reactions and subsequent workups were carried out under an argon environment. All reagents were used as received.

$[Mo_2(mhp)_2(CH_3CN)_4][BF_4]_2$

To a solution of 0.624 g (1 mmol) of $Mo_2(mhp)_4$ in 30 mL acetonitrile was added 4.5 mL of a 1 M solution of Et_3OBF_4 (Et = ethyl) in dichloromethane. The mixture was stirred at 70 °C for 2 h and then for an additional 24 h at room temperature. The solution was reduced in volume and toluene was slowly added until a precipitate formed. The solid product was collected on a frit and washed with 15 mL of toluene. 0.437 g of product was recovered.

$[^nBu_4N]_2[O_2CC_6F_4CO_2]_2$

Preparation was analogous to the aforementioned dicarboxylate salt preparations.

Reaction of $[Mo_2(mhp)_2(CH_3CN)_4][BF_4]_2$ and $[^nBu_4N]_2[O_2CC_6F_4CO_2]$

A solution of 0.387 g (0.60 mmol) $[^nBu_4N]_2[O_2CC_6F_4CO_2]_2$ in 75 mL of acetonitrile was added to a solution of 0.400g (0.60 mmol) of $[Mo_2(mhp)_2(CH_3CN)_4][BF_4]_2$ in 75 mL acetonitrile at an approximate rate of 10 mL per minute. The solution immediately turned from blue to dark red in color with a precipitate forming halfway through the addition. The precipitate was collected on a frit and washed three times with acetonitrile (15 mL total) and once with hexanes (5 mL), then dried under vacuum. The reaction yielded 0.207 g of a red solid. By MALDI-TOF mass spectrometry this was shown to be a mixture of dimers of dimers, $[Mo_2(mhp)_3]_2\ [O_2CC_6F_4CO_2]$, molecular triangles $[Mo_2(mhp)_3]_3\ [O_2CC_6F_4CO_2]_3$, and molecular squares, $[Mo_2(mhp)_3]_4\ [O_2CC_6F_4CO_2]_4$.

REFERENCES

(1) Cotton, F. A.; Harris, C. B. *Inorg. Chem.* **1965**, *4*, 330.

(2) Chisholm, M. H.; Macintosh, A.M. *Chemical Reviews.* **2005**, 105, 2549.

(3) Chisholm, M. H. *Acc. Chem. Res.* **2000,** 33, 53.

(4) Cotton, F. A.; Walton, R. A. *Multiple Bonds between Metal Atoms*; Clarendon Press: Oxford, 1993.

(5) Cotton, F. A.; Donahue, J. P.; Lin, C.; Murillo, C. A. *Inorg. Chem.* **2001**, *40*, 1234.

(6) Chisholm, M. H. *J. Organ. Chem.* **2002**, *641*, 15.

(7) Kondo, H.; Yamaguchi, Y.; Nagashima, H. *J. Am. Chem. Soc.* **2001**, *123*, 500.

(8) Kincaid, K.; Gerlach, C. P.; Giesbrecht, G. R.; Hagadorn, J. R. *Organometallics* **1999**, *18*, 5360.

(9) Cotton, F. A.; Lin, C.; Murillo, C. A. *Inorg. Chem.* **2001**, *40*, 472.

(10) Cotton, F. A.; Daniels, L. M.; Lin, C.; Murillo, C. A. *J. Am. Chem. Soc.* **1999**, *121*, 4538.

(11) Cotton, F. A.; Donahue, J. P.; Murillo, C. A. *J. Am. Chem. Soc.* **2003**, *125*, 5436.

(12) Cotton, F. A.; Wang, W. *Inorg. Chem.* **1984**, *23*, 1604.

(13) Cotton, F. A.; Wilkinson, G.; Murillo, C. A.; Bochmann, M. *Advanced Inorganic Chemistry*; 6th ed.; John Wiley & Sons, Inc.: New York, 1993.

(14) Cotton, F. A.; Lin, C.; Murillo, C. A. *Acc. Chem. Res.* **2001**, *34*, 759.

(15) Cotton, F.A.; Fanwick, P.E.; Niswander, R.H.; Sekutowski, J.C. *J. Chem. Am. Soc.* **1978**, *100*, 4725.

(16) Cayton, R.H.; Chisholm, M.H.; Putilina, E.T.; Folting, K.; Huffman, J.C.; Moodley, K.G. *Inorg. Chem.* **1992**, *31*, 2928.

(17) Cayton, R.H.; Chisholm, M.H.; Huffman,J.C.; Lobkovsky, E.B. *J. Am. Chem. Soc.* **1991**, *113*, 8709.

(18) Bursten, B.E.; Chisholm, M.H.; Hadad, C.M.; Li, J.; Wilson, P.J. *Chem. Commun,* **2001**, 2382.

(19) Chisholm, M.H.; Patmore, N.J. *The Chemical Record.* **2005,** *5*, 308.

(20) Brown, D.J; Chisholm, M.H. Unpublished results